

## Article

# Effect of a Tetraethoxysilane Hydrolysis Reaction Catalyst on the Precipitation of Hydrolysis Products in the Pores of a Polyimide Track Membrane

Natalia Igorevna Cherkashina \*, Vyacheslav Ivanovich Pavlenko, Semen Nikolayevich Domarev and Nikolay Valeriyevich Kashibadze

Department of Theoretical and Applied Chemistry, Belgorod State Technological University Named after V.G. Shukhov, 308012 Belgorod, Russia; belpavlenko@mail.ru (V.I.P.); domarev542@gmail.com (S.N.D.); bel-liteyshik@yandex.ru (N.V.K.)

\* Correspondence: cherkashina.ni@bstu.ru

**Abstract:** This paper presents the results of obtaining a composite film based on polyimide track membranes filled with a silica filler, although the issue of the deposition of this filler in the pores of the given membranes remained unexplored. The filler was obtained by hydrolysis of tetraethoxysilane using an alkaline and acid catalyst. This paper presents the results of the effect of the tetraethoxysilane hydrolysis reaction catalyst on the precipitation of hydrolysis products in the pores of the polyimide track membrane. The factors influencing the formation of silicon oxide nanofibers within the matrix template (polyimide track membrane) are determined. It was found that the use of an acid catalyst provides the highest rates of filling, while when using an alkaline catalyst, the filling is practically not observed, and only single pores are filled. The properties of the composite film obtained were investigated. SEM images of the surface and chip of the composite while using alkaline and acid catalyst are presented. The spatial structure of composite films based on track membranes was investigated by FTIR spectroscopy. The hydrolysis of tetraethoxysilane in an acid medium significantly decreases the optical density index of the membranes and simultaneously increases their light transmission index. The greatest changes are observed in the range of 500–1000 nm, and there are no detectable changes in the range of 340–500 nm. When using an alkaline catalyst, there is not the same significant decrease in the relative optical density index D.

**Keywords:** hydrolysis; composite film; track membrane; silicon oxide; nanotubes



**Citation:** Cherkashina, N.I.; Pavlenko, V.I.; Domarev, S.N.; Kashibadze, N.V. Effect of a Tetraethoxysilane Hydrolysis Reaction Catalyst on the Precipitation of Hydrolysis Products in the Pores of a Polyimide Track Membrane. *ChemEngineering* **2023**, *7*, 32. <https://doi.org/10.3390/chemengineering7020032>

Academic Editor: Alirio E. Rodrigues

Received: 7 March 2023

Revised: 5 April 2023

Accepted: 6 April 2023

Published: 10 April 2023



**Copyright:** © 2023 by the authors. Licensee MDPI, Basel, Switzerland. This article is an open access article distributed under the terms and conditions of the Creative Commons Attribution (CC BY) license (<https://creativecommons.org/licenses/by/4.0/>).

## 1. Introduction

The production of nanosystems based on high-purity silicon oxide, as well as precipitation of silicon oxide on various substrates, has a number of practical applications. These applications range from creating mesoporous adsorbents and nanofilters to obtaining antireflective coatings on optical glass [1–4]. In addition to the abovementioned applications of such systems, it is of great interest to study the properties of the composite polymeric materials filled with them. For example, treatment with vacuum ultraviolet ( $\lambda = 90\text{--}115\text{ nm}$ ) of a polymer composite based on high-impact polystyrene and organosiloxane filler increases the solar radiation absorption by  $\sim 15\%$ , which was noted in the corresponding study [5].

While creating filled compositions, including polymeric ones, there is one essential restriction, which is the impossibility of introducing a significant amount of functional filler without the composite losing its strength characteristics. This restriction can be successfully eliminated by modifying the surface of the filler with various modifiers, including those containing silicon oxide [6,7]. In terms of quality, such systems significantly differ from their unmodified counterparts [8]. However, this solution is only applicable for polymer compositions—in which the filler is introduced before the polymer matrix is formed, such

as in the method of hot pressing—or if it is necessary to introduce a significant amount of filler (more than 10% vol).

Polyimide track membranes are films in which there are many through pores, most often cylindrical and of the same size [9–11]. There are a number of works in which the creation of polymeric composites was carried out by deposition of metal salts in pores of polymer nuclear membranes [12,13], although the issue of deposition of silica filler in the pores of the given membranes remains unexplored.

In the case of an existing polymer matrix template, such as a track membrane, it is necessary to form the filler directly within the template or to obtain the filler of a strictly defined size for its subsequent introduction into the template. Theoretically, this technology has an advantage over volumetric composite molding, namely, the relative uniformity of filler distribution in the volume of the matrix. The uniformity of filler distribution in the volume of the matrix plays an important role if a small amount of filler needs to be introduced [14–16].

In most cases, the synthesis of silica fillers for composite systems is implemented by the sol-gel method with the use of a catalyst to accelerate the process [17–19]. In the process of silica filler production, the base catalyst is most often used due to the fact that it provides the necessary dynamics of the sol-gel system during tetraethoxysilane (TEOS) hydrolysis to form spherical structures of a regular shape [20,21]. In addition to the change in system viscosity (sol-gel transition), the resulting structure of the polycondensation reaction products significantly differs. Thus, a linear polymer is formed in an acid medium, while a branched cluster is formed in a base medium [22].

The most commonly used method for obtaining structures of this class is the Stöber process [23], which is represented by the growth of new layers around the core seeds. In general, the process is represented by layer-by-layer growth of silicon oxide particles on the surface of the primary nucleus, in some cases, the synthesis homogeneously proceeds in one stage, but a multistage variation of this method—which allows the synthesis of highly spherical silicon dioxide-based nanostructures by heterogeneous synthesis—is also widely studied. With a sufficiently accurate selection of the parameters of this process, including the introduction of cyclohexane molecules at the first stage to create seeds (heterogeneous synthesis), it is possible to obtain monomodal systems of spherical nanostructures in the size range of 20–100 nm with a size deviation of ~5% [20]. The technology of silicon dioxide nanofibers production using electrospinning for their formation is also known [3,4]. It is noteworthy that the resulting nanofibers are represented by mesoporous silica gel with a spherical space unit [24].

The paper presents a method used to synthesize nanostructures of high-purity silica filler used for the modification of polymer composite based on a polyimide track membrane. The purpose of the work was to study the effect of the catalyst of the TEOS hydrolysis reaction on the precipitation of hydrolysis products in the pores of a polyimide track membrane to create a SiO<sub>2</sub>-filled composite film.

## 2. Materials and Methods

### 2.1. Synthesis of Silica Filler in Acid and Alkaline Media

A polyimide track (nuclear) membrane was used as a polymer matrix template. The SEM image of the membrane is shown in Figure 1.

The pore density of the Belgian (it4ip, Belgium) commercial track polyimide membrane was  $5 \times 10^8 \text{ cm}^{-1}$ . With an average pore size of 200 nm, their degree of filling is  $\approx 1.57\%$  vol, with the polymer  $\approx 98.43\%$  vol.

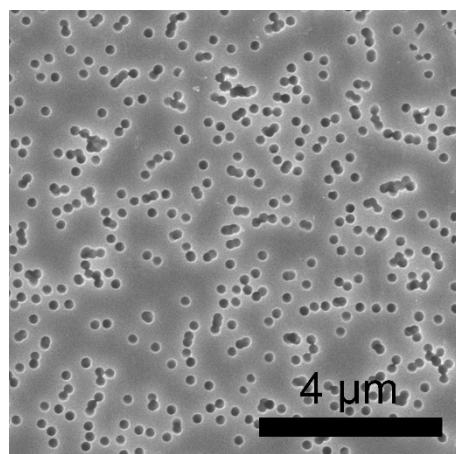
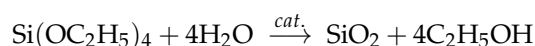


**Figure 1.** The SEM image of the polyimide track (nuclear) membrane.

The following chemical reagents were used to produce the silica filler: TEOS (produced by EKOS-1 JSC, Russia), distilled (deionized) water, ammonium hydroxide 25% (Sigma-Aldrich<sup>®</sup>, Merck KGaA, Darmstadt, Germany), and 96% acetic acid (Sigma-Aldrich<sup>®</sup>, Merck KGaA, Darmstadt, Germany).

The process of silica filler production in a general form can be expressed in the form of a reaction, which in the case of complete flow is as follows:



Synthesis of the  $\text{SiO}_2$  filler was carried out in glass beakers with a lid with a total volume of the reaction mixture of 49.4 mL for each unit of glassware. The choice of this type of glassware was due to the necessity of placing the track membranes in them with their subsequent removal for drying. Because aqueous solutions of acids and bases do not mix well with TEOS, the first stage of hydrolysis (1.5 h) was performed with constant active stirring and heating of the reaction medium using an ultrasonic homogenizer (20 kHz, 60 °C). This allowed for a uniform distribution of the reagents throughout the reaction volume and an increase in the area of the contact boundary (aqueous medium—TEOS), which greatly affects the rate of the hydrolysis reaction.

An acidic hydrolysis medium was obtained by adding an aqueous acid solution per one mole of TEOS. The required reagents were premixed in a molar ratio of 2.46( $\text{H}_2\text{O}$ ):0.012(acetic acid) to obtain a reaction mixture with  $\text{pH} \approx 3$ .

To obtain an alkaline hydrolysis medium per one mole of TEOS, the necessary components were also premixed in the molar ratio 2.46( $\text{H}_2\text{O}$ ):0.016( $\text{NH}_4\text{OH}$ ) to obtain a reaction mixture with  $\text{pH} \approx 11$ . The synthesis, analogous to acid hydrolysis, was performed in glass beakers with a lid and a total volume of the reaction mixture of 49.4 mL.

## 2.2. Membrane Treatment

Polyimide track membranes were pretreated with concentrated TEOS by placing them in the abovementioned alkoxide for 30 min under constant exposure to 20 kHz ultrasound and 20 W radiant power. This step was necessary to remove air from the pores. TEOS was chosen because PI track membranes are better wetted with non-polar liquids (contact angle for water  $\approx 70 \pm 5^\circ$ , diiodomethane  $\approx 40 \pm 5$ ). After the saturation of the membranes was completed, aqueous solutions of acid and base catalysts were introduced into the reaction volume, followed by the first stage of hydrolysis.

At the end of the first stage of hydrolysis, the membranes were extracted and washed in deionized water, followed by drying at 20 °C for one day. For the control samples, the light transmission spectrum was recorded, followed by a 1-h microwave treatment of the membranes at a frequency of 2450 Hz with a radiation power of 800 W. This step was

necessary to effectively remove bound water and unreacted reagents from the silica filler obtained in the pores [25].

### 2.3. Research Method

The light transmission spectra of the track polyimide membranes were obtained using a LEKI SS1207 spectrophotometer (Finland). The spectral range of the spectrophotometer is from 325 to 1000 nm. The accuracy of the wavelength setting is  $\pm 2$  nm.

In order to determine the spatial structure of the obtained composite film (polymer composite), we studied FTIR spectra obtained on a VERTEX 70 FTIR spectrometer (Bruker, Ettlingen, Germany).

X-ray powder diffractograms were obtained using ARL X'TRA (Thermo Fisher Scientific SARL, Ecublens, Switzerland).

A Being BV-50L vacuum drying oven (Being Instrument, Shanghai, China) was used for heat treatment.

Microwave treatment was performed using a NuWav-Pro microwave workstation (Nutech Analytical, Kolkata, India) at 800 W.

Ultrasonic treatment was performed using an ultrasonic laboratory unit (dispersant) II100-840 (Inlab Ultrasound LLC, St. Petersburg, Russia).

## 3. Results and Discussion

### 3.1. Spectrum of Light Transmission of Composites Based on Polyimide Track Membranes

Figure 2 shows the light transmission spectra of polyimide track membranes. The relative density index was set according to air ( $D = 0$ ). The spectra for the membranes were recorded twice—before the microwave treatment and after that. The images were recorded in wavelength increments of 20 nm.

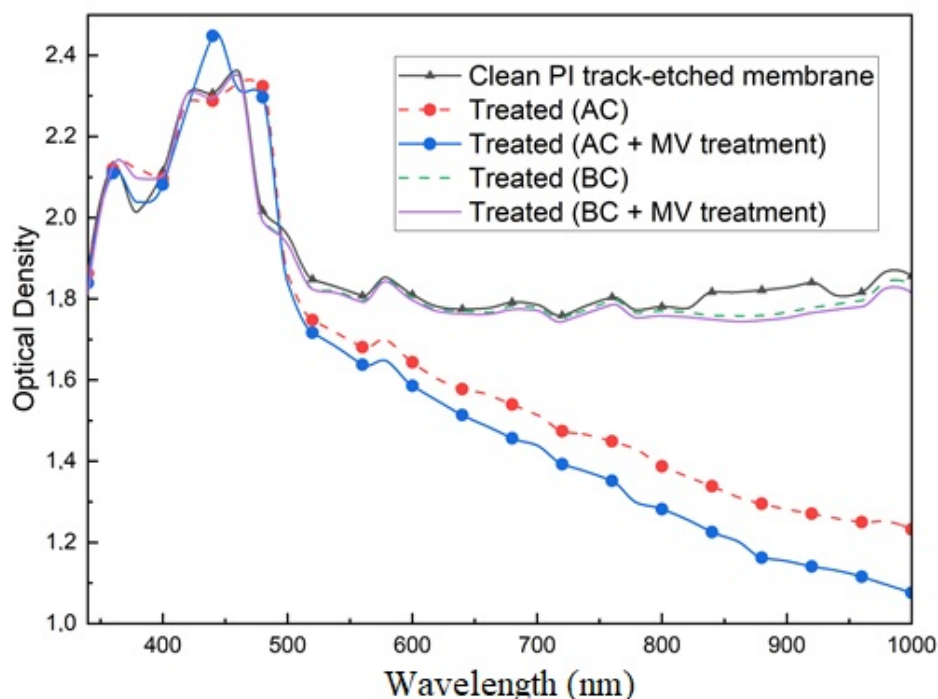


**Figure 2.** Changes in the optical density index of track membranes when treated with products: AC—hydrolysis with acid catalyst; AC + MV treatment—hydrolysis with acid catalyst followed by microwave treatment; BC—Hydrolysis with base catalyst; BC + MV treatment—hydrolysis with base catalyst followed by microwave treatment.

It is worth noting that the graphs have one common feature. In both cases, after hydrolysis and microwaves the spectra of the membranes show different parts, which

closely replicate the features of the characteristic spectrum of a pure polyimide membrane. This property indicates the preservation of the porous structure of the track membrane.

As can be seen from the graphs shown in Figure 2, the TEOS hydrolysis in an acid medium significantly reduces the optical density index of the membranes and, simultaneously, increases their light transmission index. The greatest changes are observed in the range of 500–1000 nm, which corresponds to the long- and medium-wavelength range of the visible spectrum. In turn, in the 340–500 nm range, there are no detectable changes, and the membrane spectrum is characterized by a close-to-the-average spectrum of pure polyimide track membranes (Figure 2 line with triangular markers).

The decrease in the optical density of membranes after acid hydrolysis indicates the presence of SiO<sub>2</sub>. Silica nanofiller has an amorphous structure, which makes its optical properties similar to glass. Due to the formation of silica fibers in the membrane, light-conducting channels appear in the pores. In untreated membranes, part of the light flux is absorbed due to the non-perpendicular orientation of the pores, in the case of a treated membrane, this part of the light flux freely passes through.

The slight decrease in optical density of microwave-treated membranes most likely indicates the presence of hydrolysis products as well as unreacted TEOS and water in the nanofibrous filler. These liquids have different refractive indices, which are considerably higher than those of air, and their removal from the silica filler expectedly leads to a decrease in optical density. It is important to point out that after 1 h of microwave treatment, the surface temperature of the membranes was  $142 \pm 5$  °C, which corresponds to the heating temperature of a pure polyimide membrane. It is most likely that the heating of polyimide membranes after microwave exposure is primarily due to the water content in both samples, in the case of the pure polyimide membrane, it is adsorbed from the air.

Figure 2 also shows the transmission spectra of the track polyimide membrane, the hydrolysis of the filler for this membrane was carried out with an alkaline catalyst. In contrast to the first variant of hydrolysis with an acidic catalyst, these membranes do not show the same significant decrease in the relative optical density *D*. The changes of this parameter are very small compared with the pure membrane and are within the range of variation of the given parameter for different samples of membranes. As in the first case, microwave treatment also leads to a slight decrease in the relative optical density within the wavelength range from 720 to 1000 nm, but these changes can also be considered insignificant.

As further studies have shown, the most complete removal of residual TEOS hydrolysis products using both acidic and basic catalysts can be achieved by subjecting the films to microwave treatment at  $250 \pm 5$  °C for one hour, or by increasing the microwave treatment time to 3 h in the same mode. The removal of residual products of TEOS hydrolysis after microwave treatment is confirmed by EDX data (Figure 3). Atoms Si, O, and C were fixed in the silica filler before microwave treatment (Figure 3a). After microwave treatment, there is no further change in the optical density index for the track membrane samples and no traces of TEOS are detected within the silica filler, as indicated by the EDX spectra (Figure 3b).

Trace amounts of metallic chromium are detected due to the fact that, for EDX, it is applied as a coating on the surface of the sample (Figure 3).

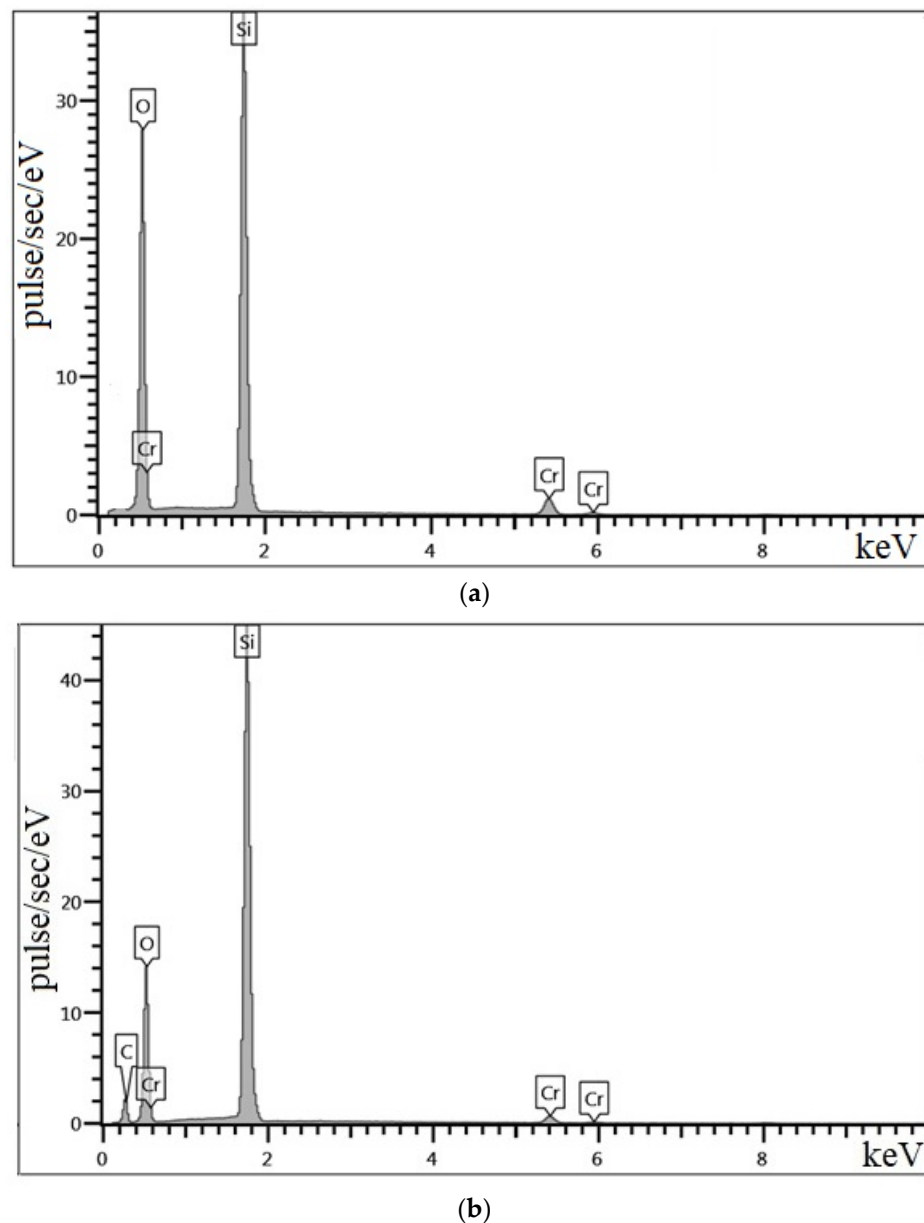


**Figure 3.** The EDX spectra of silica filler: (a) before microwave treatment and (b) after microwave treatment.

### 3.2. FTIR Spectroscopy of Composites Based on Polyimide Track Membranes

To determine the content of hydrolysis products in the pores of the track polyimide membrane, FTIR spectra were analyzed for the clean and treated samples.

Figure 4 shows the FTIR absorption spectra for the membranes treated in different hydrolysis media followed by microwave treatment. The spectra of the pure polyimide track membrane and the membrane after treatment with hydrolysis products in an acid medium are also presented for comparison. The spectrum of the membrane after treatment with hydrolysis products with the base catalyst was not included in the following graph because it completely corresponds to the spectrum of the same membrane after microwave treatment according to the abovementioned procedure.

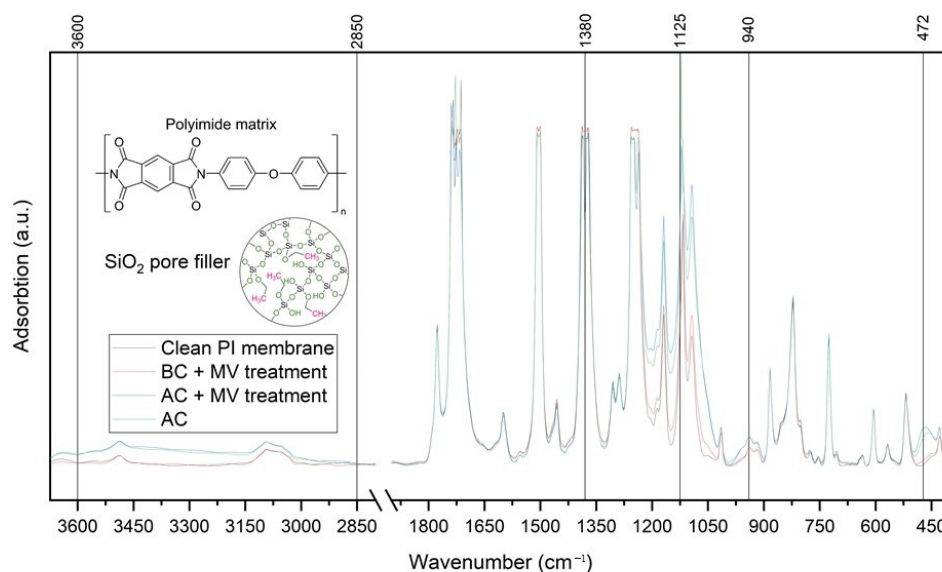


**Figure 4.** FTIR spectra of composite films based on track membranes.

Table 1 presents the interpretation of the IR spectra of the track polyimide membranes considered in the work. Based on the IR spectra data and their interpretation, it can be noted that the treatment of the films with products of TEOS hydrolysis with acid catalyst significantly increases the peak at  $\approx 1125\text{ cm}^{-1}$ , which, in addition to  $\delta\delta$  C-C and  $\delta_{ip}$  C-H vibrations in the benzene ring in the corresponding bands clearly belonging to the polyimide membrane itself, is characteristic of organosilicon compounds (e.g., TEOS) and appears during the binding of Si-O-C ethoxy groups. In addition, there is an obvious increase in the absorption coefficient in the  $2800\text{--}3700\text{ cm}^{-1}$  band, which corresponds to several compounds at once (O-H, valence longitudinal Si-OH, and  $\text{H}_2\text{O}$ ). Minor peaks in this band are observed both in the hydrolysis products and directly in the pure polyimide membrane, but in the membrane, they most probably belong only to the vibrations of  $\text{H}_2\text{O}$  adsorbed from air-bound water in the pores. When considering the peak at  $\approx 1125\text{ cm}^{-1}$ , the complex structure of the silica filler (Figure 4  $\text{SiO}_2$  pore filler) should also be taken into account. The structure of the filler also contains a certain amount of Si-O-C ethoxy groups. Thus, we can conclude that the significant enhancement of the absorption coefficient of the above band and peaks are explained by the presence of reagents and products of the hydrolysis reaction in the pores, in particular,  $\text{SiO}_2$  filler, water, and unreacted TEOS.

**Table 1.** Interpretation of IR spectra of track polyimide membranes treated with products of acidic and alkaline catalysts hydrolysis of TEOS.

Component	Vibration Frequency, $\text{cm}^{-1}$	
Polyimide	$\nu$ C-O	1320–1210
	Unflat $\delta$ OH	1020–890
	$\delta_{oop}$ OH	750–650
	$\nu_{as}$ C=O in imides	1790–1740
	$\nu_s$ C=O in imides	1730–1690
	Skeletal $\nu$ C-C in the benzene ring	1530–1475
	$\delta$ C-C	1125–1090
	$\delta_{ip}$ C-H in the benzene ring	1250–950
	$\delta_{oop}$ C-H in the benzene ring	900–690
	$\nu$ C-N polyimides	1390–1360
	$\nu$ Ar-O-Ar	1290–1230
	Amide IV $\delta$ O=C-N interaction of $\nu$ C-N and $\nu$ C=O	$\approx 620$

Table 1. Cont.

Component	Vibration Frequency, $\text{cm}^{-1}$	
Silica compounds and hydrolysis products	Si-OH	$\approx 472$
	Si-O-Si	$\approx 940$
	When binding ethoxy groups Si-O-C	$\approx 1120$
	Valence symmetric Si-O-Si	$\approx 1045$
	Asymmetric vibrations of bridging oxygen Si-O-Si	$\approx 1080$
	Valence C-O	$\approx 1170$
	Deformation symmetric $\text{CH}_3$	$\approx 1380$
	Deformation asymmetric $\text{CH}_3$ , scissors $\text{CH}_2$	$\approx 1455$
	Deformation H-O-H	$\approx 1650$
O-H, valence longitudinal Si-OH, $\text{H}_2\text{O}$	3490–3100	

Considering the  $1390\text{--}1360\text{ cm}^{-1}$  band, one can also note the enhancement of the peak at  $1380\text{ cm}^{-1}$  for films after their treatment with TEOS hydrolysis products. This absorption band in polyimides (blue line in Figure 4) corresponds to the  $\nu$  C-N bond, and for the pure film sample, this band is characterized by a doublet with peaks at  $1380\text{ cm}^{-1}$  and  $1372\text{ cm}^{-1}$ . However, after treatment, the above doublet is smoothed to a band with approximately equal intensity throughout its length due to the enhancement of the peak at  $1380\text{ cm}^{-1}$ , corresponding to  $\text{CH}_3$  deformation symmetric vibrations. In view of the fact that the intensity of this peak does not decrease after heat treatment, this circumstance also indicates some content of hydrolysis products, including the silica filler precipitated in the membranes.

The presence of the silica filler in the membrane tracks can also be judged from the separate parts of the IR spectra. In the range from  $400$  to  $1000\text{ cm}^{-1}$ , relative enhancement of two peaks at once is detected, a peak at  $472\text{ cm}^{-1}$  and a peak at  $940\text{ cm}^{-1}$ , related to the deformation vibrations of Si-OH and Si-O-Si, respectively [26]. These bonds are not present in TEOS molecules and are present only in the products of its complete and partial hydrolysis with the formation of a silica filler with a branched structure.

### 3.3. X-ray Phase Analysis of Silica Filler

In addition, the silica filler obtained as a result of the experiment was studied. Figure 5 shows the diffractograms of the silica filler powders immediately after hydrolysis (drying in a  $120 \pm 5\text{ }^\circ\text{C}$  desiccator for 2 h) and treated for 1 h with a microwave frequency of  $2450\text{ Hz}$  and a radiation power of  $800\text{ W}$ .

It is evident from the diffractograms that microwave treatment and the presence of the template matrix do not cause obvious changes in the structure of the silica filler substance recorded by this method of study. For all four samples, the diffractograms are characterized by an amorphous halo with a broad peak within the  $2\theta$  area from  $17.5^\circ$  to  $30^\circ$ , which is characteristic of amorphous silica filler [27–29].

For silica fillers, the relative degree of crystallinity was estimated by a modified Segal method [30,31] using the following formula:

$$CI_{(XDR)} = \frac{\text{Area of crystalline domain}}{\text{Area of total domain}} \cdot 100\%$$

When evaluated by this method, the final index of crystallinity can significantly vary depending on the width of the selected range corresponding to the crystalline peak. With respect to the four samples presented in the study, the range of relative crystallinity index values are as follows: AC— $40 \pm 5\%$ ; AC + MV treatment— $35 \pm 5\%$ ; BC— $38 \pm 5\%$ ; BC + MV treatment— $39 \pm 5\%$ . The indicated intervals of changes in the crystallinity index value overlap and, as a consequence, the difference between them can be considered insignificant. The presented relative crystallinity index values are within  $40 \pm 5\%$ , which in general is typical for systems with a predominance of an amorphous phase when assessing the crystallinity index using this method.

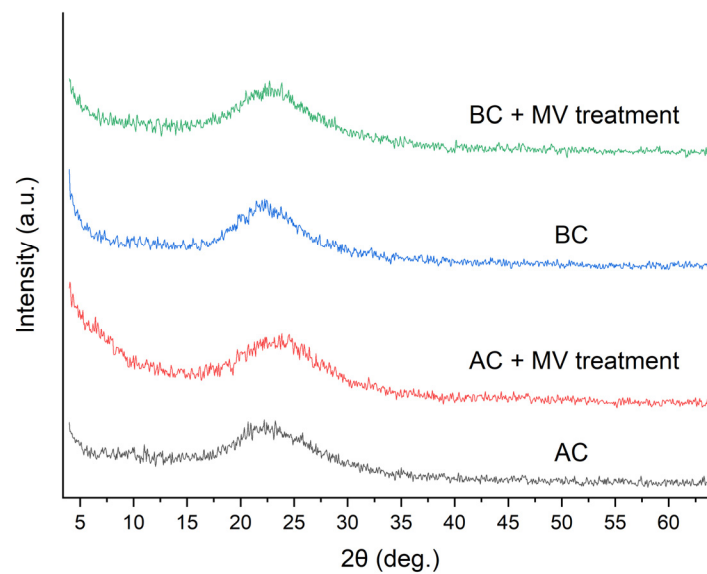


**Figure 5.** Diffractograms of silica filler: AC—hydrolysis with acid catalyst; AC + MV treatment—hydrolysis with acid catalyst followed by microwave treatment; BC—Hydrolysis with base catalyst; BC + MV treatment—hydrolysis with base catalyst followed by microwave treatment.

### 3.4. Study of the Degree of Pore Filling

In order to study the obtained nanostructures and the degree of pore filling with silica filler, the membrane sample images were obtained for hydrolysis with different catalysts.

SEM images show a significant difference in the degree of pore filling depending on the catalyst used in the hydrolysis process. Thus, the use of an acidic catalyst provides the highest rates of filling (Figure 6a), while the use of an alkaline catalyst shows almost no filling and only single pores are filled (Figure 6b). In the micrographs, the different degrees of filling are reflected by the color change of the pores from gray, when the pore is filled, to dark gray or black, when the pore is not filled.

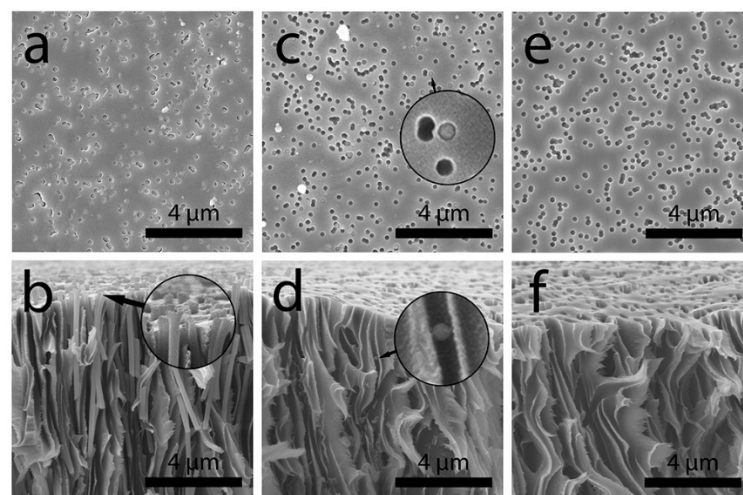


**Figure 6.** Microphotographs of the surface and chip of the track polyimide membrane: (a,b) hydrolysis with acidic catalyst followed by microwave treatment; (c,d) hydrolysis with base catalyst followed by microwave treatment; (e,f) clean track-etched polyimide membrane.

In addition to the different degrees of pore filling, it should also be pointed out that there is a significant difference in the type of nanostructures obtained. During hydrolysis with an acid catalyst, fibrous nanostructures that appear to resemble  $\text{SiO}_2$  nanofibers

described in studies [3,4] are formed. It is most likely that in these structures the unit cells are represented by spherical particles and the resulting structure is mesoporous. This assumption is confirmed by studies of similar structures, as well as the presence of single nanospheres marked in the microphotographs.

In turn, base-catalyzed hydrolysis results in a system containing strictly spherical particles and their aggregates of irregular shape [20,21]. Some of these particles are still precipitated in the pores of the track polyimide membrane, but their number is small, and there are usually 1–3 nanoparticles per filled pore. It is also worth noting that the precipitation of nanospheres in the pores occurs at different depths and, as a consequence, in some pores, the particles may be at a considerable distance from the surface of the material, which may hinder their detection (zoomed in part on Figure 6d).

#### 4. Conclusions

This paper presents the results of studies on the effect of the catalyst of the TEOS hydrolysis reaction on the precipitation of hydrolysis products in the pores of a polyimide track membrane to create a SiO<sub>2</sub>-filled polymer composite. It was found that the use of an acidic catalyst provides the highest rates of filling and leads to the formation of nanofibrous structures in pores. Due to the uncomplicated scalability and ease of implementation of the proposed method, it can be used as the basis of industrial technology for the production of SiO<sub>2</sub>-filled polymer composites.

**Author Contributions:** Conceptualization, N.I.C. and V.I.P.; methodology, validation, N.I.C. and V.I.P.; formal analysis, N.I.C.; investigation, S.N.D. and N.V.K.; writing—original draft preparation, S.N.D.; writing—review and editing, N.V.K.; supervision, N.I.C.; funding acquisition, N.I.C. All authors have read and agreed to the published version of the manuscript.

**Funding:** The work is realized using equipment of the High Technology Center at BSTU named after V.G. Shukhov the framework of the project of the Russian Science Foundation №19-79-10064 (extension). <https://rscf.ru/project/19-79-10064/> (accessed on 7 March 2023).

**Data Availability Statement:** Data sharing not applicable.

**Conflicts of Interest:** The authors declare no conflict of interest. The funders had no role in the design of the study; in the collection, analyses, or interpretation of data; in the writing of the manuscript, or in the decision to publish the results.

#### References

1. Mane, S.M.; Raorane, C.J.; Shin, J.C. Synthesis of Mesoporous Silica Adsorbent Modified with Mercapto-Amine Groups for Selective Adsorption of Cu<sup>2+</sup> Ion from Aqueous Solution. *Nanomaterials* **2022**, *12*, 3232. [[CrossRef](#)] [[PubMed](#)]
2. Es'kin, S.V.; Kosobudskii, I.D.; Zhimalov, A.B.; Ushakov, N.M.; Kul'batskii, D.M.; German, S.V.; Muzalev, P.A. Antireflecting coatings for glass based on monolayers of amorphous silica nanoparticles. *Glass Phys. Chem.* **2013**, *39*, 409–413. [[CrossRef](#)]
3. Shahhosseininia, M.; Bazgir, S.; Joupari, M.D. Fabrication and investigation of silica nanofibers via electrospinning. *Mater. Sci. Eng.* **2018**, *91*, 502–511. [[CrossRef](#)] [[PubMed](#)]
4. Choi, S.S.; Lee, S.G.; Im, S.S.; Kim, S.H.; Joo, Y.L. Silica nanofibers from electrospinning/sol-gel process. *J. Mater. Sci. Lett.* **2003**, *22*, 891–893. [[CrossRef](#)]
5. Pavlenko, V.I.; Zabolotny, V.T.; Cherkashina, N.I.; Edamenko, O.D. Effect of vacuum ultraviolet on the surface properties of high-filled polymer composites. *Inorg. Mater. Appl. Res.* **2014**, *5*, 2219–2231. [[CrossRef](#)]
6. Pavlenko, V.I.; Cherkashina, N.I. Synthesis of hydrophobic filler for polymer composites. *Int. J. Eng. Technol.* **2018**, *7*, 493–495. [[CrossRef](#)]
7. Yastrebinsky, R.N.; Pavlenko, V.I.; Matukhin, P.V.; Cherkashina, N.I.; Kuprieva, O.V. Modifying the surface of iron-oxide minerals with organic and inorganic modifiers. *Middle East J. Sci. Res.* **2013**, *18*, 1455–1462.
8. Matyukhin, P.V.; Pavlenko, V.I.; Yastrebinsky, R.N.; Cherkashina, N.I. The high-energy radiation effect on the modified iron-containing composite material. *Middle East J. Sci. Res.* **2013**, *17*, 1343–1349.
9. Awad, E.M.; Hassan, S.; Bebers, E.; Rammah, Y.S. Strong etching investigation on PADC CR-39 as a thick track membrane with deep depth profile study. *Radiat. Phys. Chem.* **2020**, *177*, 109104. [[CrossRef](#)]
10. Apel, P.Y.; Blonskaya, I.V.; Ivanov, O.M.; Kristavchuk, O.V.; Nechaev, A.N.; Olejniczak, K.; Orelovich, O.L.; Polezhaeva, O.A.; Dmitriev, S.N. Do the soft-etched and UV-track membranes actually have uniform cylindrical subnanometer channels? *Radiat. Phys. Chem.* **2022**, *198*, 110266. [[CrossRef](#)]

11. Yadegari, A.; Gohs, U.; Khonakdar, H.-A.; Wagenknecht, U. Influence of post-irradiation conditions on crosslinking and oxidation of microporous polyethylene membrane. *Radiat. Phys. Chem.* **2022**, *193*, 109997. [[CrossRef](#)]
12. Cherkashina, N.I.; Pavlenko, V.I.; Noskov, A.V.; Shkaplerov, A.N.; Kuritsyn, A.A.; Popova, E.V.; Zaitsev, S.V.; Kuprieva, O.V.; Kashibadze, N.V. Synthesis of PI/POSS nanocomposite films based on track nuclear membranes and assessment of their resistance to oxygen plasma flow. *Polymer* **2021**, *212*, 123192. [[CrossRef](#)]
13. Cherkashina, N.I.; Pavlenko, V.I.; Noskov, A.V.; Bondarenko, N.I.; Kuprieva, O.V.; Kashibadze, N.V.; Sidelnikov, R.V.; Klopot, E.P. Gamma radiation attenuation characteristics of composites based on polyimide track membranes filled with nanodispersed Pb. *Prog. Nucl. Energy* **2021**, *141*, 103959. [[CrossRef](#)]
14. Sienkiewicz, A.; Czub, P.A. Method of Managing Waste Oak Flour as a Biocomponent for Obtaining Composites Based on Modified Soybean Oil. *Materials* **2022**, *15*, 7737. [[CrossRef](#)]
15. Yang, Z.; Kang, G.; Liu, R.; Chen, P. Predicting the mechanical behaviour of highly particle-filled polymer composites using the nonlinear finite element method. *Compos. Struct.* **2022**, *286*, 115275. [[CrossRef](#)]
16. Olszewski, A.; Nowak, P.; Kosmela, P.; Piszczyk, Ł. Characterization of Highly Filled Glass Fiber/Carbon Fiber Polyurethane Composites with the Addition of Bio-Polyol Obtained through Biomass Liquefaction. *Materials* **2021**, *14*, 1391. [[CrossRef](#)] [[PubMed](#)]
17. Alhadhrami, A.; Mohamed, G.G.; Sadek, A.H.; Ismail, S.H.; Ebnalwaled, A.A.; Almalki, A.S.A. Behavior of Silica Nanoparticles Synthesized from Rice Husk Ash by the Sol–Gel Method as a Photocatalytic and Antibacterial Agent. *Materials* **2022**, *15*, 8211. [[CrossRef](#)]
18. Vorotyntsev, A.V.; Markov, A.N.; Kapinos, A.A.; Petukhov, A.N.; Pryakhina, V.I.; Nyuchev, A.V.; Atlaskina, M.E.; Andronova, A.A.; Markova, E.A.; Vorotyntsev, V.M. Synthesis and comparative characterization of functionalized nanoporous silica obtained from tetrachloro- and tetraethoxysilane by a sol-gel method. *Phosphorus Sulfur Silicon Relat. Elem.* **2021**, *196*, 176–188. [[CrossRef](#)]
19. Bokov, D.O.; Jalil, A.T.; Chupradit, S.; Suksatan, W.; Ansari, M.J.; Shewael, I.H.; Valiev, G.H.; Kianfar, E. Nanomaterial by Sol-Gel Method: Synthesis and Application. *Adv. Mater. Sci. Eng.* **2021**, *2021*, 5102014. [[CrossRef](#)]
20. Masalov, V.M.; Sukhinina, N.S.; Emel'chenko, G.A. Colloidal particles of silicon dioxide for the formation of opal-like structures. *Phys. Solid State* **2011**, *53*, 1135–1139. [[CrossRef](#)]
21. Han, Y.; Lu, Z.; Teng, Z.; Liang, J.; Guo, Z.; Wang, D.; Han, M.Y.; Yang, W. Unraveling the Growth Mechanism of Silica Particles in the Stöber Method: In Situ Seeded Growth Model. *Langmuir* **2017**, *33*, 5879–5890. [[CrossRef](#)] [[PubMed](#)]
22. Bashir, S.; Hina, M.; Iqbal, J.; Rajpar, A.H.; Mujtaba, M.A.; Alghamdi, N.A.; Wageh, S.; Ramesh, K.; Ramesh, S. Fundamental Concepts of Hydrogels: Synthesis, Properties, and Their Applications. *Polymers* **2020**, *12*, 2702. [[CrossRef](#)] [[PubMed](#)]
23. Stöber, W.; Fink, A.; Bohn, E. Controlled growth of monodisperse silica spheres in the micron size range. *J. Colloid Interface Sci.* **1968**, *26*, 62–69. [[CrossRef](#)]
24. Lee, D.J.; Lee, H.; Ryou, M.H.; Han, G.B.; Lee, J.N.; Song, J.; Choi, J.; Cho, K.Y.; Lee, Y.M.; Park, J.K. Electrospun Three-Dimensional Mesoporous Silicon Nanofibers as an Anode Material for High-Performance Lithium Secondary Batteries. *ACS Appl. Mater. Interfaces* **2013**, *5*, 12005–12010. [[CrossRef](#)]
25. Pickles, C.; Lu, T. Microwave Dewatering of Gibbsite-Type Bauxite Ores: Permittivities, Heating Behavior and Strength Indices. *Minerals* **2022**, *12*, 648. [[CrossRef](#)]
26. Rubio, F.; Rubio, J.; Oteo, J.L. A FT-IR study of the hydrolysis of Tetraethylorthosilicate (TEOS). *Spectrosc. Lett.* **1998**, *31*, 199–219. [[CrossRef](#)]
27. Potapov, V.V.; Fediuk, R.S.; Gorev, D.S. Obtaining sols, gels and mesoporous nanopowders of hydrothermal nanosilica. *J. Sol-Gel Sci. Technol.* **2020**, *94*, 681–694. [[CrossRef](#)]
28. Purnawira, B.; Purwaningsih, H.; Ervianto, Y.; Pratiwi, V.M.; Susanti, D.; Rochiem, R.; Purniawan, A. Synthesis and characterization of mesoporous silica nanoparticles (MSNp) MCM 41 from natural waste rice husk. *IOP Conf. Ser. Mater. Sci. Eng.* **2019**, *541*, 012018. [[CrossRef](#)]
29. Verma, J.; Bhattacharya, A. Analysis on Synthesis of Silica Nanoparticles and its Effect on Growth of *T. Harzianum* & *Rhizoctonia* Species. *Biomed. J. Sci. Tech. Res.* **2018**, *10*, 7890–7897. [[CrossRef](#)]
30. Segal, L.; Creely, J.J.; Martin, A.E.; Conrad, C.M. An Empirical Method for Estimating the Degree of Crystallinity of Native Cellulose Using the X-Ray Diffractometer. *Text. Res. J.* **2016**, *29*, 786–794. [[CrossRef](#)]
31. Rotaru, R.; Savin, M.; Tudorachi, N.; Peptu, C.; Samoila, P.; Sacarescu, L.; Harabagiu, V. Ferromagnetic iron oxide–cellulose nanocomposites prepared by ultrasonication. *Polym. Chem.* **2018**, *9*, 860–868. [[CrossRef](#)]

**Disclaimer/Publisher's Note:** The statements, opinions and data contained in all publications are solely those of the individual author(s) and contributor(s) and not of MDPI and/or the editor(s). MDPI and/or the editor(s) disclaim responsibility for any injury to people or property resulting from any ideas, methods, instructions or products referred to in the content.